MRI VENTILATION ANALYSIS BY MERGING PARAMETRIC ACTIVE CONTOURS

Nilanjan Ray[1], Scott T. Acton[1], Talissa Altes[2] and Eduard E. de Lange[2]

[1]Department of Electrical and Computer Engineering, University of Virginia, Charlottesville, VA 22904
[2]Department of Radiology, University of Virginia, Charlottesville, VA 22908
{nray, acton, taa2c, eed6s}@virginia.edu

ABSTRACT

A novel technique that combines MR imaging of hyperpolarized helium gas and conventional MR imaging facilitates high resolution imaging of lung functionality for the first time. In this paper, we put forth a segmentation method for measuring the total lung air space and a classification approach to computing the functional air space. For segmentation, we introduce a parametric active contour that allows automated merging of multiple contours. The active contour technique uses gradient vector flow modified and strengthened by a boundary condition that inhibits contour crossover. The active contour approach is computationally inexpensive and is independent of initial contour placement. For classification of the functional lung air space in the helium images, a fuzzy c-means technique is applied. The classification results, in conjunction with the segmentation, allow the analysis of ventilation. The resultant biomedical image analysis tool will be used in determining the efficacy of certain respiratory treatments.

1. INTRODUCTION

Recently, innovative technology has made possible the analysis of ventilation by way of magnetic resonance imaging (MRI). MRI examination with hyperpolarized ^{3}He gas as a contrast agent is emerging as a potential tool among medical researchers attempting to quantify lung functionality and the effect of respiratory-related drugs [1]. In this paper we provide a segmentation technique for determining total lung air space. The analysis depends upon the information from two modalities a) Proton images (^{1}H MRI) that reveal the lung cavity and b) Helium images (MRI imagery where ^{3}He is inhaled) showing the ventilated portions of the lungs. Figure 1 shows one 2-D slice of the proton imagery, and Figure 2 shows the corresponding ^{3}He slice. So, to quantify the functional lung air space, we quantitatively compare the volume extracted from the proton imagery and the volume extracted from the helium imagery.

From a biomedical perspective, this effort is the first to quantify ventilation from MRI data. Traditional ^{1}H MRI does not capture lung functionality, since the concentration of ^{1}H nuclei in lung water vapor is low. So, until the introduction of the Helium-based MRI analysis [1], clinical imaging of lung parenchyma was performed using x-ray computed tomography, ventilation scintigraphy, and chest radiography. The x-ray approach sometimes uses xenon gas as a contrast agent, and the scintigraphy approach uses radioactive gases or aerosols. With an MRI-based approach, the exposure to radioactive contrast agents is eliminated, and the poor resolution associated with the xenon-based approach is avoided.

The novelty of this work, from an image processing perspective, lies in the active contour technique used to capture the total lung cavity space from the proton imagery. It is well known that parametric active contours [2] have lower associated computational complexity compared to the geometric counterpart [3]. Also, parametric active contours, or snakes, are more easily controlled in terms of rigidity and elasticity. Geometric active contours tend to create gaps where weak image features or weak image edges exist [4]. On the other hand, the main disadvantage associated with parametric active contours is the difficulty in merging or splitting. With geometric contours, the processes of splitting and merging are inherent [3]. McInerney and Terzopolous first reported merging and splitting of parametric active contours in [5]. In each iteration of their contour evolution method, additional operations must be implemented a) to evaluate the conditions of merging or splitting, b) to compute which portions of the contour must be merged, and c) to subsequently re-parameterize the contours. These operations involve computing the points of intersection of the snake with the sides of the triangles in a superimposed triangular grid. If one grid zone is cut by more than one snake, splitting or merging is required. The computation of the conditions and remedies for contour merging and splitting adds to the computational cost of evolving the contour.

In contrast, the proposed method eliminates any such explicit computation to merge two or more growing snakes that are initially non-intersecting. In fact, the cost of merging is identical to the cost of a non-merging scenario. At the end of the contour evolution, we merely delete the common boundaries that exist.

After the lung cavity volume is determined from merging active contours on the proton imagery, we compute the volume of functional lung air space from the helium imagery. A fuzzy *c*-means classification is used to locate the functional regions in the helium imagery.

In the remainder of this paper, we give an overview of parametric snakes (Section 2) and discuss the proposed technique for merging parametric snakes (Section 3). Section 4 compares the proposed technique with other

0-7803-6725-1/01/$10.00 ©2001 IEEE

current active contour evolution methods, and Section 5 demonstrates the application of the method to ^{1}He images and shows the classification of the ^{3}He imagery.

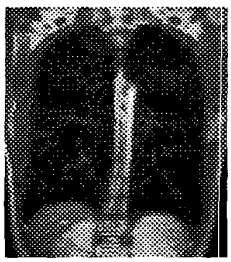

Figure 1. Proton image

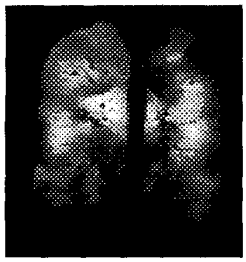

Figure 2. Helium image

2. PARAMETRIC ACTIVE CONTOURS

A 'snake' or 'active contour' is a curve defined on the rectangular image domain. A snake can move on this domain by the influence of internal and external forces. The internal force is typically the resistance to bending and stretching of the snake itself. The external forces are computed from the image data and are often so defined that the snake conforms to object edges. A *parametric* active contour or snake is a parametric curve $\mathbf{C}(s)=(p(s), q(s))$, $s\in[0,1]$ that attempts to minimize an energy functional [2,6,7]:

$$E_s = \int_0^1 \left(\frac{1}{2} \left\{ \alpha |\mathbf{C}'(s)|^2 + \beta |\mathbf{C}''(s)|^2 \right\} + E_{ext}(\mathbf{C}(s)) \right) ds, \qquad (1)$$

where the first term in the integral represents internal energy of the snake, and E_{ext} represents the external energy term. The non-negative constants α and β of the internal energy term represent the resistance to stretching and that to bending of the active contour, respectively. $\mathbf{C}'$ and $\mathbf{C}''$ denote the first and the second derivative of the curve with respect to the parameter s. The external energy term E_{ext} may be expressed by $-|\nabla G_\sigma(x,y) * I(x,y)|$, defined as the *edge map* in [6], where $I(x,y)$ is the image intensity at location (x, y), $G_\sigma(x,y)$ is two dimensional Gaussian kernel with standard deviation σ and ∇ is the gradient operator. The energy functional (1) is minimized by the variational principle to obtain following Euler equation:

$$\alpha\mathbf{C}''(s) - \beta\mathbf{C}''''(s) - \nabla E_{ext}(\mathbf{C}(s)) = 0 \qquad (2)$$

where $\mathbf{C}''$ and $\mathbf{C}''''$ are the 2nd and 4th derivatives of the curve with respect to the parameter s. We may consider (2) as a force-balance equation where the external force is $-\nabla E_{ext}(\mathbf{C}(s))$ [6]. In order to solve (2), the snake is treated a function of time t, as well as the parameter s, *i.e.*, $\mathbf{C}(s,t)$. Then the partial derivative of $\mathbf{C}$ with respect to time t is computed using:

$$\mathbf{C}_t(s,t) = \alpha\mathbf{C}''(s,t) - \beta\mathbf{C}''''(s,t) + \mathbf{v}(\mathbf{C}(s,t)) \qquad (3)$$

where $\mathbf{v}$ is the external force. When the solution $\mathbf{C}(s,t)$ stabilizes, the term $\mathbf{C}_t(s, t)$ goes to zero. The success of this technique depends on the design of the external force $\mathbf{v}$ by which the snake is guided.

3. MERGING ACTIVE CONTOURS

To develop a technique for automatic merging of the active contours, we desire a well-motivated implicit approach that does not involve significant additional processing. In this context, we have designed the external force term in such a way that two non-intersecting as well as growing active contours never cross each other. The initial active contours are treated as sources emitting unit normal vectors on the image domain. The force $\mathbf{v}$ in (3) is computed by diffusing these normal vectors along with the image edge force, which attracts the snake toward object boundary. In order to do so, we have taken the process as the diffusion defining a Generalized Gradient Vector Flow (GGVF)[7]. The GGVF has some attractive properties for snake evolution, such as its ability to guide the snake into long, thin cavities. Another useful property is that the GGVF equation converges to non-trivial solution unlike the isotropic diffusion counterpart. The GGVF equation is defined as follows [7]:

$$\mathbf{v}_t = g(|\nabla f|)\nabla^2\mathbf{v} - h(|\nabla f|)(\mathbf{v} - \nabla f) \qquad (4)$$

where ∇^2 is the Laplacian operator. The functions g and h are defined as

$$g(|\nabla f|) = e^{-(|\nabla f|/K)}, \quad h(|\nabla f|) = 1 - g(|\nabla f|), \qquad (5)$$

where K is a user defined parameter controlling the degree of smoothness of $\mathbf{v}$ and $f(x,y)$ is defined as the "edge map" and is equal to $|\nabla G_\sigma(x,y) * I(x,y)|$ for gray level images [6]. We solve equation (4) with adding a boundary condition as follows:

$$\mathbf{v} = \text{unit outward normal on } \partial D, \qquad (6)$$

where ∂D is representing the initial snake boundaries.

Thus, we diffuse the gradients of the edge map and the outward normal vectors defined on the initial snakes. Owing to the competitive nature of the diffusion process, the field $\mathbf{v}$ is constructed in such a way that between two or more growing snakes there is a separating streamline. So, the growing snakes moving under the influence of $\mathbf{v}$ never cross each other. Instead, the snake stops at its interface with a competing snake, giving the desired effect – the merging of parametric snakes.

To make this point clear we have taken a simple synthetic circle image and placed three initial snakes within it as seen from Figure 3. Figure 4 depicts the evolution of snakes on the image, and Figure 5 shows the same result after removal of the common boundary, yielding a final result. For this example, the field $\mathbf{v}$ is given in Figure 6. One can clearly observe that between two growing snakes there is always a separating

streamline where the field **v** terminates from two sides of this streamline. Two growing snakes terminate at these streamlines and hence never cross each other.

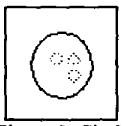
Figure 3. Circle with initial snakes

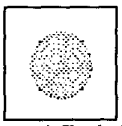
Figure 4. Evolution process


Figure 5. Final result of evolution

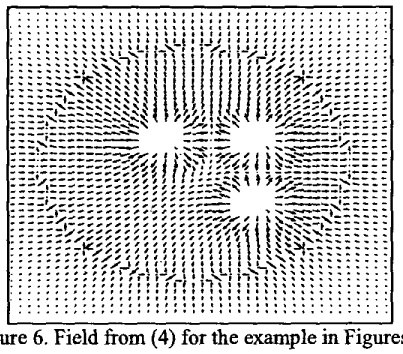
Figure 6. Field from (4) for the example in Figures 4-5.

4. COMPARISON WITH OTHER TECHNIQUES

The proposed method of diffusion is superior to the original GGVF with respect to the initial snake placement within objects. Figure 7 shows the same circle image with one initial snake. Figure 8 and 9 give the standard GGVF snake evolution and the proposed snake evolution sequence. This example reveals the sensitivity of the standard GGVF algorithm to initial snake placement. The reason for this sensitivity is that the GGVF flow defines a medial axis [8], and so the initial snake must include the medial axis in order to capture the desired object. The only constraint in case of the proposed flow is that the object should include all the snakes, but the snakes themselves do not need to include the medial axis.

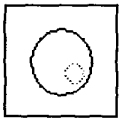
Figure 7. Circle with initial snake

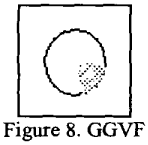
Figure 8. GGVF snake evolution


Figure 9. Proposed evolution process

Other active contour methods such as the pressure force [9], the distance force [6] and the GGVF (or GVF) [6,7] are incapable of automatically merging snakes. In fact, these methods allow the overlapping of snakes that collide in evolution. The proposed method closely resembles the pressure snake [9], except that it prevents overlapping. More importantly, the pressure snake suffers from a lack of control over stopping at weak edges [6]. The proposed method overcomes this difficulty as well, since the underlying diffusion process is a GGVF.

5. APPLICATION TO LUNG VENTILATION DETERMINATION

The target application of the proposed active contour method is total lung cavity volume calculation. The ratio of volume computed from the helium imagery (yielding functional volume) and the cavity volume computed from the proton imagery can be used to calculate percent ventilation. This ratio can be used as a measure of the efficacy of certain pulmonary drugs. To determine total lung volume, initial snakes (circular in shape) are placed inside the cavity (the dark region in Figure 1). Here the proposed method is advantageous over GGVF, because it alleviates the need include the medial axis of the lung cavity, a requirement that would be difficult to automate for each MRI slice.

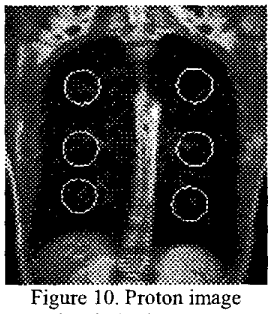
Figure 10. Proton image with six initial snakes

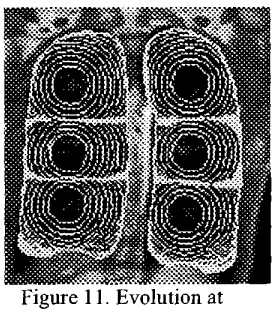
Figure 11. Evolution at an intermediate stage

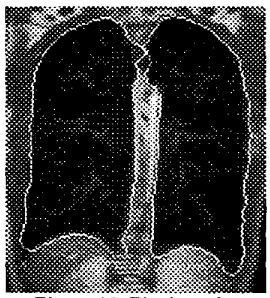
Figure 12. Final result showing total lung space


Figure 13. Fuzzy *c*-means classification of Helium image

Figure 10 shows the initial snakes placed within the proton image of Figure 1, and Figure 11 presents the evolution process. Multiple snakes aid the evolution process in two ways: (1) the localized snakes decrease the overall edge localization error, and (2) the multiple snakes are able to evolve in parallel saving evolution time when compared to the single snake approach. The final result, after removal of common boundaries, is given in Figure

12. By comparing to ground truth data obtained from the UVa. School of Medicine, we can assess the accuracy of this volume computation.

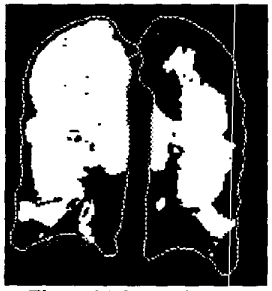

Figure 14. Lung air space from pre-treatment imaging

Figure 15. Lung air space from post-treatment imaging

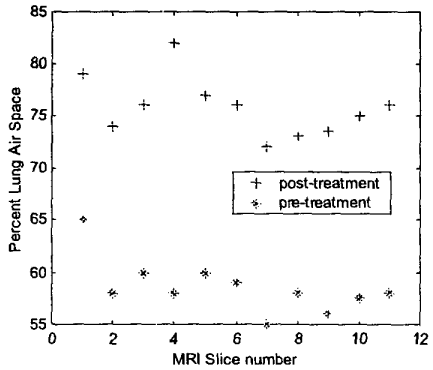

Figure 16. Improvement on percent lung air space.

After computing the lung cavity volume from the proton imagery with the active contour method, we compute the functional lung air space from the ^{3}He imagery. We take the final evolved snake contours from proton image slice and register them to the corresponding helium image slice. We then classify the zone of the helium image slice that is within the computed contour into three classes (as directed by the UVa medical researchers for these images) by fuzzy *c*-means [10]. The classification is unsupervised and is performed on the original unprocessed data. An example classification is shown in Figure 13. The two classes with higher associated mean intensity values are combined to form the lung air space as shown in Figure 14. Now the functional lung air space ratio is calculated as the ratio of lung air space to total lung space. Figure 15 shows lung air space obtained on a post-treatment proton image slice. Figures 13-15 also show the overlaid contours.

To process the entire set of volumetric slices for one patient, the set of proton MRI slices is processed in conjunction with the corresponding set of ^{3}He MRI slices. We have calculated the functional lung air space ratio for each of the slice both in post and pre-treatment scenarios and have plotted the comparative graphs in Figure 16. From this graph, the efficacy of the treatment may be observed.

6. CONCLUSION

We have designed a novel technique for merging parametric active contours and have successfully applied the technique to MRI data for the purpose of ventilation analysis. In our future research we aim to extend the technique to both merging and splitting without increasing the computational burden.

Acknowledgements: We thank Dr. Jack Knight-Scott of UVa. Biomedical Engineering for advice and direction in processing MR imaging.

7. REFERENCES

[1] E.E. de Lange, J.P. Mugler, III, J.R. Brookeman, J. Knight-Scott, J. Truwit, C.D. Teates, T.M. Daniel, P.L. Bogorad and G.D. Cates, "Lung air spaces: MR imaging evaluation with hyperpolarized ^{3}He gas." *Radiology*, vol. 210, pp. 851-857, 1999.

[2] M. Kass, A. Witkin and D Terzopolous, "Snakes: Active contour models," *Int. Jour. Comput. Vis.*, vol. 1, pp. 321-331, 1987.

[3] J.A. Sethian, *Level set methods and fast marching methods.* Cambridge:Cambridge University Press, 1999.

[4] C. Xu, A. Yezzi, J.L. Prince, "On the relationship between parametric and geometric active contours." In *34th Asiomar Conference on Signals, Systems, and Computers,* Oct 29 – Nov. 1, 2000.

[5] T. McInerney and D. Terzopolous, "Topology adaptive snakes." In *5th Inetrnational Conference on Computer Vision*, pp. 840-845, Cambridge, Massachusetts, 1995.

[6] C. Xu and J.L. Prince, "Snakes, Shapes, and Gradient Vector Flow," *IEEE Trans. Image Processing*, vol. 7, pp. 359-369, 1998.

[7] C. Xu and J.L. Prince, "Generalized gradient vector flow external forces for active contours." *Signal Processing*, vol. 71, pp. 131-139, 1998.

[8] S. Osher, "Level set based algorithms for image restoration, surface interpolation and solving PDEs on general manifolds with applications to image processing and computer graphics." In *34th Asiomar Conference on Signals, Systems, and Computers*, Oct 29 – Nov. 1, 2000.

[9] L.D. Cohen, "On active contour models and balloons." *CVGIP: Image Understanding*, vol. 53, pp. 211-218, 1991.

[10] J.C. Bezdek, J. Keller, R. Krisnapuram, N.R. Pal, *Fuzzy models and algorithms for pattern recognition and image processing.* Boston: Kluwer Academic Publisher, 1999.